BME 590: Rehabilitation Robotics

Final Project

Alexander Kyu

I. Introduction

Upper limb exoskeletons have been significant in a number of roles. In the instance of rehabilitation, these devices such as the exoskeleton, MAHI Exo II, from Pehlivan, et al. help people who have experienced strokes or Spinal Cord Injuries regain certain functionalities and movements in their upper extremities. This not only has significant social impacts on these people's lives, but also have significant economic impacts of over $20 billion in indirect costs alone [1].

While certainly many developing upper limb exoskeletons are meant to be used in a physician's office, there is also a lot of development around wearable exoskeletons to augment human capabilities. This can range from assistance with daily activities such as the proposed and designed exoskeleton from Sui, et al. to providing additional power to tasks like lifting heavy objects or other physical activities [2].

This project is the start to the design of a three degree-of-freedom upper limb exoskeleton used for spiking a ball. While it is quite limited and additional controls need to be implemented, this paper describes the preliminary control strategy for basic torque control.

II. Methods

First, a selected subject, Alexander Kyu, was selected and an estimated arm was modeled. This involved modeling each segment as both a conical frustum and a cylinder. This means that a maximum radius, minimum radius, average radius, and limb length were measured for this model. Finally, an assumption of a density, $\rho = 1.1$ g/cm^3, was used for all limbs. The axes for the limbs and selected conical frustum and cylinder models were determined by the Modified Denavit-Hartenberg (DH) Notation (**Figure 1**).

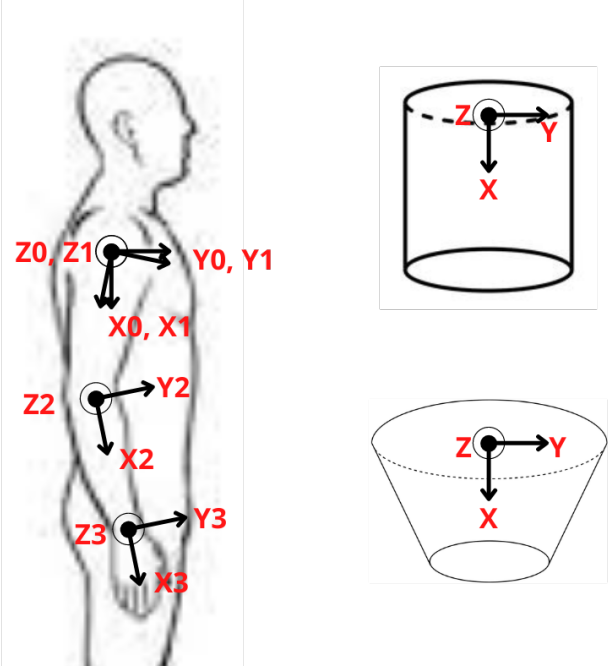

Figure 1: DH Configuration of Model and Axes for both the Cylinder and Conical Frustum Models. Note that the starting orientation of the arm is pointed downwards.

Using the conical frustum model, the center of mass along the length of the limbs was determined based on Equation (1) and the mass was determined based on Equation (2) where R_1 is the larger radius and R_2 is the smaller radius of the conical frustum.

$$X_{com\_limb} = \frac{h(R_1^2 + 2R_1R_2 + 3R_2^2)}{4(R_1^2 + R_1R_2 + R_2^2)} \quad (1)$$

$$m_{limb} = \rho * V = \rho * \frac{\pi h}{3}(R_1^2 + R_1R_2 + R_2^2) \quad (2)$$

Next, some early assumptions were made about the exoskeleton design. First, the assumed masses were 2 kg, 1 kg, and 1 kg for the upper arm, lower arm, and hand, respectively. Second, the center of masses for the exoskeleton subsections were assumed to be at the proximal ends of the limbs, so the shoulder, elbow, and wrist, respectively. Furthermore, this means the overall

center of mass and masses for each limb were changed. The corresponding masses were added to each limb and the center of masses were adjusted according to Equation (3).

$$X_{com} = \frac{X_{com\_limb} * m_{limb}}{m_{limb} + m_{exoskeleton}} \quad (3)$$

Using the cylinder model, the Moment of Inertias for each axis of each limb were calculated. The Products of Inertias were assumed to be 0 for this model. Equation (4) and Equation (5) were used to determine these Moment of Inertias for the Inertial Tensor I^C. Also, the masses of the exoskeleton subsections were ignored in these calculations because they were assumed to be point masses located at the axis rotation. Additionally, the Inertial Tensor is shown in Equation (6).

$$I_{xx} = \frac{1}{2} m_{limb} R^2 \quad (4)$$

$$I_{yy} = I_{zz} = \frac{m_{limb} R^2}{4} + \frac{m_{limb} h^2}{12} + \frac{m_{limb} h^2}{4} = \frac{m_{limb} R^2}{4} + \frac{m_{limb} h^2}{3} \quad (5)$$

$$I^C = \begin{matrix} I_{xx} & 0 & 0 \\ 0 & I_{yy} & 0 \\ 0 & 0 & I_{zz} \end{matrix} \quad (6)$$

Next, based on the coordinate system as shown in Figure 1, a Modified DH Table (**Table 1**) was created with its corresponding DH Transformation Matrices.

Link	α_{i-1}	a_{i-1}	d_i	θ_i
1	0	0	0	$\theta_{UpperArm}$
2	0	$h_{UpperArm}$	0	$\theta_{LowerArm}$
3	0	$h_{LowerArm}$	0	θ_{Hand}

Based on the given joint trajectories, the Recursive Newton-Euler Inverse Dynamics Algorithm (**Figure 2**) was used to determine joint torques required in the exoskeleton joints to obtain the desired joint trajectories.

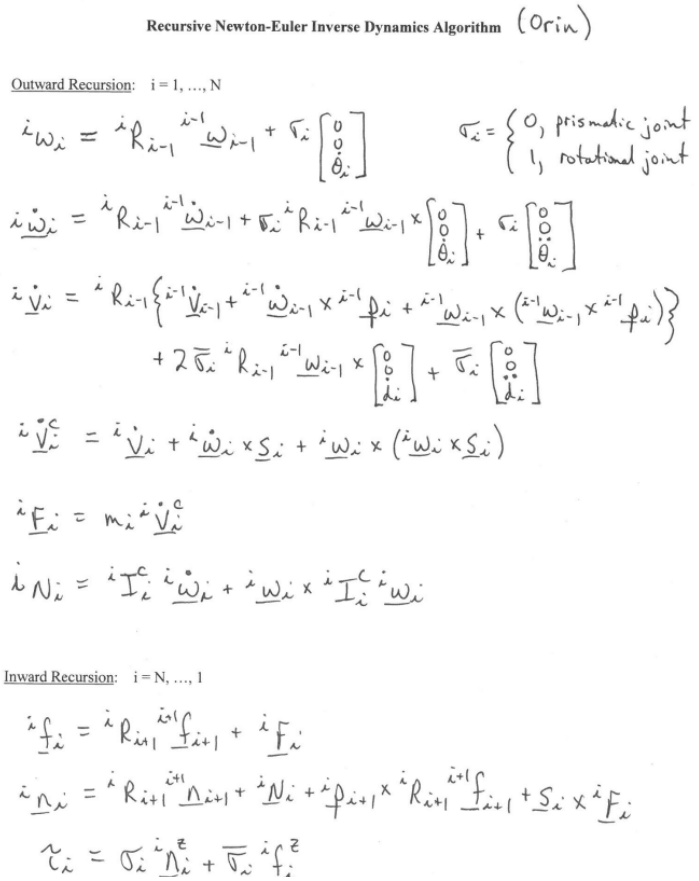

Figure 2: Recursive Newton-Euler Inverse Dynamics Algorithm used to determine joint torques.

Lastly, Working Model 2D was used to develop the simulation. A two-dimensional model of the subject's arm was created (**Figure 3**) and the associated masses, moment of inertias, lengths and widths were adjusted as described above. The calculated torques were inputted to the joints of the simulation and a ball was added to show the hand spiking it. The joint angles and joint angular velocities were recorded and compared to the desired angles and angular velocities.

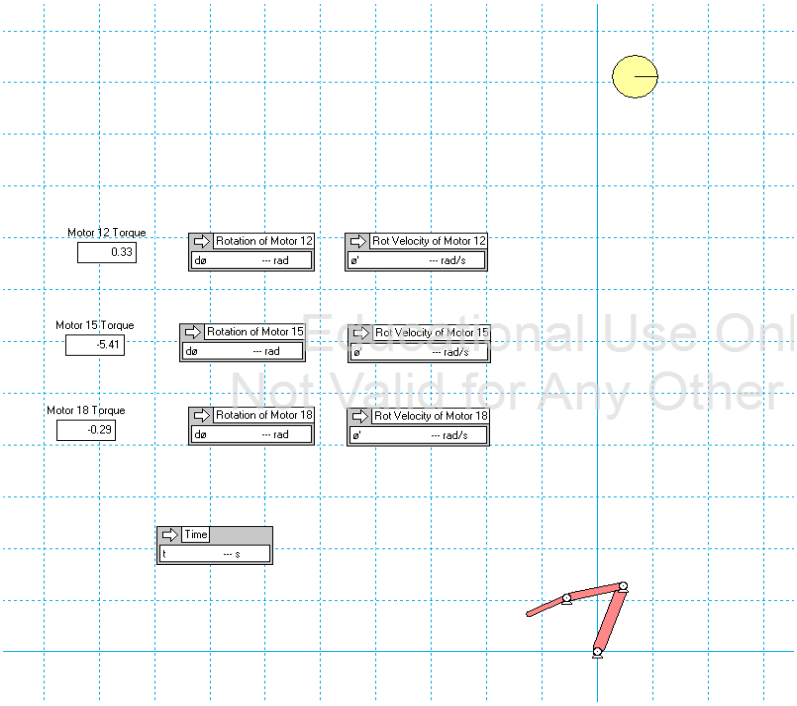

Figure 3: Working Model 2D Simulation with the modelled hand and ball.

III. Results

A graph of the calculated joint torques are shown in **Figure 4**. The upper arm had the largest magnitude and fluctuations in torque while the hand had the lowest. This correlates with the magnitude and fluctuations of the desired joint angles.

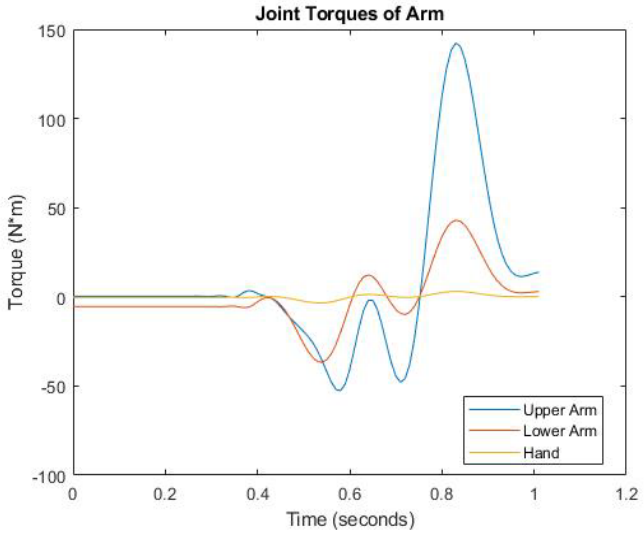

Figure 4: Calculated Joint Torques of each limb over the time of the ball spike.

Furthermore, graphs of the desired versus generated (from the joint torques) joint angles and angular velocities are shown in **Figure 5**. All generated joint angle and angular velocities are near identical to the desired values up until the time of contact with the ball around 0.6 seconds. At this point, the wrist/hand joint has the largest deviation from its desired joint angle and angular velocity. Moreover, an increase in the mass of the ball further increased the deviation between the desired and actual for all joints.

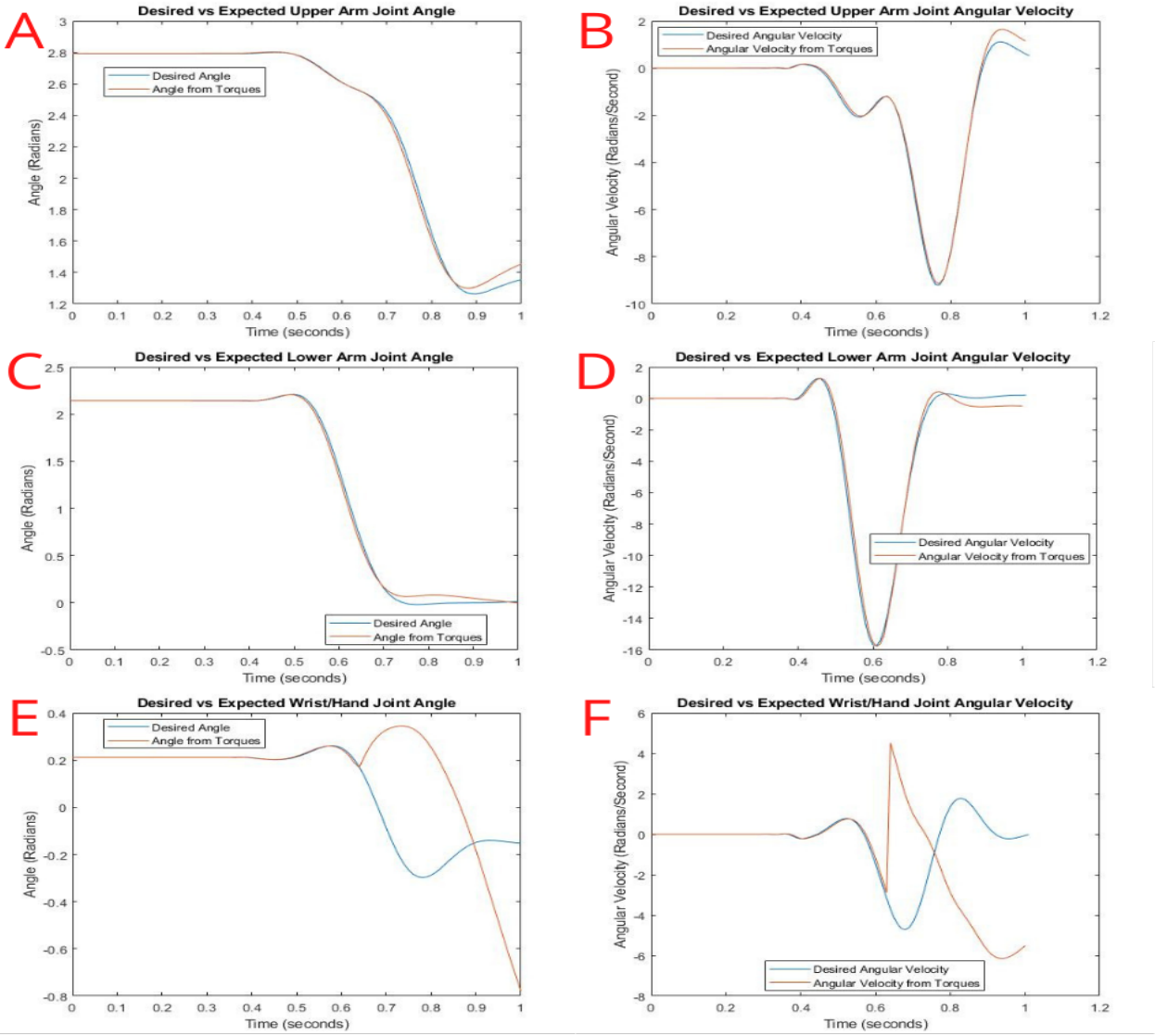

Figure 5: A) Desired versus Actual (Angle from Torques or Expected) Upper Arm Joint Angle. B) Desired versus Actual Upper Arm Angular Velocity. C) Desired versus Actual Lower Arm Joint Angle. D) Desired versus Actual Lower Arm Angular Velocity. E) Desired versus Actual Wrist/Hand Joint Angle. F) Desired versus Actual Wrist/Hand Angular Velocity.

IV. Discussion

The large deviation in the desired versus actual wrist/hand joint angle was due to the impact that the actual model had with the ball. Because the system was designed in an open-loop configuration with no consideration for the needed impact force on the ball, any external force would affect the resulting joint angles and angular velocities. Because the hand is relatively light compared to the other joints and is the joint of impact, it had the largest deviation. As stated above, the larger the mass, the higher the deviation.

As for the small deviation in all of the joints before the moment of impact, this is likely due to the fact that these simulations and calculations are done through discrete time points. Smaller time-steps would yield lower deviation and higher accuracy at the cost of increased processing time required. This is often a problem in continuous systems using discrete simulations and calculations.

This is simply one limitation of this model and simulation. Other limitations include the simplification of the model. The arm is quite complex with varying points of density and a shape that is different than a simple cylinder or conical frustum. This would also extend to the design of the exoskeleton. Furthermore, the Products of Inertia of each joint are not likely to be 0 and in a more accurately described model, would not be 0. Another limitation would be the fact that this is a two-dimensional model. An arm has quite a few more degrees-of-freedom, and in an ideal state, spiking a ball would involve those additional degrees-of-freedom to optimize movement and power. Of course, this would add complexity to the exoskeleton too, as well as the calculated model and simulation.

There is quite a bit of future work that could be done on this project. First, as mentioned before, the extension into the third dimension would add a bit of complexity, but also yield a more robust and ideal exoskeleton and model. Second, the model could increase in complexity a little bit with the chosen shapes used for limb representation and calculations around the Inertial Tensor. Third, with the introduction of external forces such as the ball, creating a closed-loop control for the torque control would limit and ideally diminish the difference between desired and actual joint angles and angular velocities introduced by external forces.

Despite the large amount of work to be done to improve this model, this early-stage simulation proved to be fairly accurate in its current limitations in the absence of external forces. Future work to account for these errors and to improve the model's accuracy are quite achievable.

V. References

[1] Pehlivan, A. U., Celik, O., & O'Malley, M. K. (2011). Mechanical design of a distal arm exoskeleton for stroke and spinal cord injury rehabilitation. *2011 IEEE International Conference on Rehabilitation Robotics*. https://doi.org/10.1109/icorr.2011.5975428

[2] Dongbao Sui, Jizhuang Fan, Hongzhe Jin, Xuefeng Cai, Jie Zhao, & Yanhe Zhu. (2017). Design of a wearable upper-limb exoskeleton for activities assistance of daily living. *2017 IEEE International Conference on Advanced Intelligent Mechatronics (AIM)*. https://doi.org/10.1109/aim.2017.8014123